Adjustments to the law of the wall above an Amazon forest explained by a spectral link

Luca Mortarini, Gabriel G. Katul, Daniela Cava, et al.

View Online   Export Citation   CrossMark

ARTICLES YOU MAY BE INTERESTED IN

Deep Learning Model for Two-Fluid Flows
Physics of Fluids (2023); https://doi.org/10.1063/5.0134421

Wake vortex structures and hydrodynamics performance of a power-extraction flapping hydrofoil
Physics of Fluids **35**, 025105 (2023); https://doi.org/10.1063/5.0133931

A review of droplet bouncing behaviors on superhydrophobic surfaces: Theory, methods, and applications
Physics of Fluids **35**, 021301 (2023); https://doi.org/10.1063/5.0136692

Physics of Fluids

Special Topic: Paint and Coating Physics

Submit Today!

Adjustments to the law of the wall above an Amazon forest explained by a spectral link

Luca Mortarini,[1] Gabriel G. Katul,[2] Daniela Cava,[3,a] Cleo Quaresma Dias-Junior,[4] Nelson Luis Dias,[5] Antonio Manzi,[6] Matthias Sorgel,[7] Alessandro Araújo,[8] and Marcelo Chamecki[9]

AFFILIATIONS

[1] Consiglio Nazionale delle Ricerche (CNR) Istituto di Scienze dell'Atmosfera e del Clima (ISAC), Torino, Italy
[2] Department of Civil and Environmental Engineering, Duke University, Durham, North Carolina 27708, USA
[3] Consiglio Nazionale delle Ricerche (CNR) Istituto di Scienze dell'Atmosfera e del Clima (ISAC), Lecce, Italy
[4] Department of Physics, Federal Institute of Pará, Belém, Brazil
[5] Department of Environmental Engineering, Federal University of Paraná, Curitiba, Brazil
[6] Instituto Nacional de Pesquisas Espaciais (INPE), Cachoeira Paulista, Brazil
[7] Atmospheric Chemistry Department, Max Planck Institute for Chemistry, Mainz, Germany
[8] Empresa Brasileira de Pesquisa Agropecuária (EMBRAPA), Belém, Brazil
[9] Department of Atmospheric and Oceanic Sciences, University of California, Los Angeles, California 90095, USA

[a] Author to whom correspondence should be addressed: d.cava@le.isac.cnr.it

ABSTRACT

Modification to the law of the wall represented by a dimensionless correction function $\phi_{RSL}(z/h)$ is derived using atmospheric turbulence measurements collected at two sites in the Amazon in near-neutral stratification, where z is the distance from the forest floor and h is the mean canopy height. The sites are the Amazon Tall Tower Observatory for $z/h \in [1, 2.3]$ and the Green Ocean Amazon (GoAmazon) site for $z/h \in [1, 1.4]$. A link between the vertical velocity spectrum $E_{ww}(k)$ (k is the longitudinal wavenumber) and ϕ_{RSL} is then established using a co-spectral budget (CSB) model interpreted by the moving-equilibrium hypothesis. The key finding is that ϕ_{RSL} is determined by the ratio of two turbulent viscosities and is given as $\nu_{t,BL}/\nu_{t,RSL}$, where $\nu_{t,RSL} = (1/A) \int_0^\infty \tau(k) E_{ww}(k) dk$, $\nu_{t,BL} = k_v(z - d)u_*$, $\tau(k)$ is a scale-dependent decorrelation time scale between velocity components, $A = C_R/(1 - C_I) = 4.5$ is predicted from the Rotta constant $C_R = 1.8$, and the iso-tropization of production constant $C_I = 3/5$ given by rapid distortion theory, k_v is the von Kármán constant, u_* is the friction velocity at the canopy top, and d is the zero-plane displacement. Because the transfer of energy across scales is conserved in $E_{ww}(k)$ and is determined by the turbulent kinetic energy dissipation rate (ε), the CSB model also predicts that ϕ_{RSL} scales with L_{BL}/L_d, where L_{BL} is the length scale of attached eddies to $z = d$, and $L_d = u_*^3/\varepsilon$ is a macro-scale dissipation length.

Published under an exclusive license by AIP Publishing. https://doi.org/10.1063/5.0135697

I. INTRODUCTION

The significance of the flow within the roughness sublayer (RSL) above tall vegetated canopies to a plethora of physical, chemical, and biological processes is not in dispute.[1–4] It suffices to note that numerical weather predictions (NWPs) and Earth system models (ESMs) require a handshake between the land surface and the atmosphere. Above tall forests such as the Amazon, this handshake occurs in the RSL whose effects on the flow are usually ignored within NWP and ESM.[5,6] The RSL delineates a region where the flow statistics are impacted by the presence of roughness elements but is below the much-studied inertial sublayer (ISL).[3,7–9]

For vegetated canopy flows, this region spans $z/h \in [1, 2-5]$[3,4,7,10] with the lower bound associated with momentum exchange and the upper bound associated with scalar exchange, where z is the distance from the ground and h is the canopy height. Hereafter, the RSL thickness from the ground is designated as z_*. Other estimates of z_* based on tree (or roughness element) spacing have also been proposed.[4,10–12]

For the mean longitudinal velocity U, the RSL effects are traditionally accommodated using a so-called roughness sublayer correction function ϕ_{RSL} so that the law of the wall,[13,14] presumed to be applicable in the ISL, is expressed as[11,15–22]

$$\frac{\kappa_v(z-d)}{u_*}\Gamma(z) = \phi_{RSL}(z/z_*, d/h, \ldots), \tag{1}$$

where $\Gamma(z) = dU/dz$ is the mean velocity gradient at z, $u_* = (\tau_s/\rho)^{1/2}$ is the friction velocity, τ_s is the turbulent stress defined at $z/h = 1$, ρ is the mean air density, $\kappa_v = 0.4$ is the von Kármán constant,[23] and d is the zero-plane displacement. Equation (1) serves as one definition of ϕ_{RSL} that allows its empirical determination with a drawback that it requires an estimate of d. Methods to estimate d are numerous[24] though the common one is the centroid of the vertically distributed drag force acting on the fluid due to the presence of obstacles.[25,26] For dense canopy flows, common values for d/h vary from 0.6 to 0.9 with higher values originating from urban canopy studies.[27,28] Notwithstanding the dependence on d, this form of ϕ_{RSL} is convenient for theoretical and practical reasons. Formulating RSL effects as an adjustment to Γ instead of U is desirable as dU/dz is Galilean invariant, whereas U is not.[29] On the practical side, extensions to stratified flow cases become convenient as ϕ_{RSL} can be framed as a generalized similarity function derived from the product of the standard form of the Monin–Obukhov[30] stability correction function and a function representing the RSL effects on Γ. Thus, $\phi_{RSL}(\cdot)$ is a dimensionless roughness sublayer modification function yet to be determined and frames the scope of the work here for near-neutral stratification. Near-neutral stratification forms a logical starting point for any extension toward stratified cases in the future. In some studies above urban canopies and permeable beds, ϕ_{RSL} has been represented as an adjustment to κ_v.[31,32] Here, the convention from vegetated canopy turbulence is followed and $\kappa_v = 0.4$ is not altered. By virtue of this definition, the log-law is recovered when $\phi_{RSL}(\cdot) = 1$ though more significant is its independence of z. For this reason, phenomenological theories describing $\phi_{RSL}(\cdot)$ assume that $\phi_{RSL}(\cdot) \to 1$ when $z \to \infty$.[4,17,18,33,34] Thus far, studies (laboratory and field) suggest enhancement in momentum transport in the RSL when compared to ISL predictions,[2–4,10,15,26,33–36] thereby requiring that $\phi_{RSL} \le 1$ (though values close to unity have been reported in the RSL as well for near-neutral stratification[16,37]). A common empirical form for ϕ_{RSL} that satisfies these minimal constraints is[4,10,17,18,33,34,38]

$$\phi_{RSL} = 1 - \exp\left[-a_1\left(\frac{z-d}{z_*}\right)\right], \tag{2}$$

where a_1 is related to the canopy roughness properties (usually encoded in a bulk drag coefficient). This formulation for ϕ_{RSL} ensures that $z_*/z_o > 1$, where z_o is the momentum roughness length (usually of order 0.1 h). In fact, some of the earliest wind tunnel studies already demonstrated that $z_*/z_o \gg 1$[39] and more recent estimates place z_*/z_o to be between 15 and 25.[4,27] Equation (2) ensures that the RSL effects diminish asymptotically with increasing $z - d$ and the log-law for U is recovered (also asymptotically) far above the canopy. Common estimates for a_1 vary from 2 to 3 and other forms for ϕ_{RSL} such as power laws [i.e., $\phi_{RSL} = (z/z_*)^n$ for $z/z_* < 1$ with $n = 0.6$[36]] have been proposed and are reviewed elsewhere.[4] To recap, in all laboratory canopy flow studies as well as numerous field experiments, $\phi_{RSL} < 1$, and this finding is opposite to what is reported for impervious walls where $\phi_{RSL} > 1$.[40] Extending the log-law to near the canopy top leads to an underestimate of measured U but an overestimate of U in the RSL over impervious walls. It is the effect on ϕ_{RSL} that

distinguishes the RSL of canopy flows from canonical rough-wall boundary layers.

While the structure of turbulence in the RSL above tall canopies has been extensively studied,[3,7,41] what appears missing is a connection between $\phi_{RSL}(.)$ and the most prominent feature of the flow ϕ_{RSL} proclaims to describe—turbulent energetics (or fluctuations) carried by eddies of all sizes. The time is ripe to undertake this connection given the recent advances in understanding the spectral properties of RSL in the atmosphere above vegetated canopies.[42] Early work on ϕ_{RSL} speculated that wake-diffusion is responsible for $\phi_{RSL} < 1$[43] though this speculation was displaced by the so-called mixing layer (ML) analogy for dense canopies.[35] Attempts to include the vorticity thickness or shear length scale (L_s) associated with ML eddies in the description of ϕ_{RSL} have already been proposed.[24,26,33] These descriptions associate a single (and fastest) growing mode of instability (Kelvin–Helmholtz type) leading to coherent structures to be the dominant effective mixing-length in the RSL, thereby ignoring all other energetic modes in the spectrum of turbulence that contribute to momentum fluxes.[35] Interestingly, that U has an inflection point at $z/h = 1$, which was already documented as early as 1926 in a tropical forest in Panama.[44] However, the connection to Kelvin–Helmholtz instabilities and coherent structures transporting momentum above canopies took some 70 yr to develop. While conventional mixing length theories attribute a single mixing length to momentum transport, RSL turbulence involves multiple length scales prompting interest in how to accommodate all of them in the estimation of ϕ_{RSL}. The work here seeks to arrive at a description of $\phi_{RSL}(.)$ starting from the energetics of turbulence whereby all eddy sizes contribute to momentum transport. The data sets used in this exploration have been collected at two sites. The first is the Amazon Tall Tower Observatory (ATTO, 1), which spans up to $z/h \in [1, 8]$ though the focus on near-neutral stratification precludes the use of all of these heights. The second is the Green Ocean Amazon (GoAmazon), which spans $z/h \in [1, 1.4]$. The data from GoAmazon were collected at a tower (ZF2) situated in the Cuieiras Biological Reserve some 60 km north–northwest of the city of Manaus, Amazonas, Brazil. The ATTO site is situated in the central Amazon rainforest of Brazil within a pristine forested area unaffected by deforestation or other human interferences. Prior work at the ATTO site precluded the onset of an ISL and argued instead that the outer layer and RSL dominate the flow statistics and specifically called for new methods to be developed to correct ISL similarity arguments.[45] It was also shown that in some cases, ISL scaling appears to hold for certain flow statistics but not others.[46] However, among the variables used to argue against the existence of the ISL are the statistics of the vertical velocity variance.[45] The vertical velocity variance appears to deviate from its expected ISL scaling at heights further away above the canopy top but is closer to ISL scaling within the RSL[47] inconsistent with logical expectations.[45] Others have argued that the presence of gentle topography can lead to substantial distortions to the turbulent kinetic energy (K) budget and introduce lack of equilibrium required to the attainment of the ISL.[48] Moreover, over the past decade, a number of studies have proposed the use of a so-called dissipation length scale L_d to represent flow statistics in the RSL and ISL alike. The L_d collapses to $\kappa_v(z - d)$ in the ISL when production (P_m) and dissipation (ε) of K are balanced and when $\phi_{RSL} = 1$.[49–52] Thus, L_d may be another appropriate length scale to include in the description of ϕ_{RSL} and has not traditionally been considered in many prior RSL studies (with

some notable exceptions[24,50–52]). Hence, the work here seeks to explore all these connections by addressing two inter-related questions: (i) What are the links between the spectral properties of turbulence and ϕ_{RSL}? (ii) Is there a formal relation between ϕ_{RSL} and L_d deviating from $\kappa_v(z - d)$? These questions are answered using near-neutral stratification runs collected at ATTO and GoAmazon and analyzed from a co-spectral budget (CSB) model.[53,54]

II. THEORY

Three models for ϕ_{RSL} are proposed and compared to Eq. (1) at ATTO and GoAmazon. The first uses a simplified turbulent momentum flux budget along with standard closure schemes (Sec. II C). The second uses a "spectral" version of the same approach and establishes a link between ϕ_{RSL} and the spectrum of the vertical velocity (Sec. II D). The third adopts idealized shapes for the spectrum of vertical velocity in the RSL,[42] thereby enabling an analytical link between ϕ_{RSL} and L_d (Sec. II E). However, before presenting these models, key concepts and definitions are reviewed for completeness.

A. Definitions

The Cartesian coordinate system used defines x, y, and z along the longitudinal, lateral, and vertical directions, respectively, with $z = 0$ being the ground or forest floor, and the longitudinal direction is along the mean wind direction. The instantaneous velocity components along x, y, and z directions are labeled as u, v, and w, respectively, with $U = \bar{u}$ defining the mean velocity, and overline is time averaging. Turbulent fluctuations from their time-averaged values are indicated by primed quantities with $\overline{w'u'}$ being the turbulent momentum flux at z, $\sigma_u = \sqrt{\overline{u'u'}}$, $\sigma_v = \sqrt{\overline{v'v'}}$, and $\sigma_w = \sqrt{\overline{w'w'}}$ being the root-mean squared velocity fluctuations along the x, y, and z directions, respectively. The turbulent kinetic energy is defined here as $K = (1/2)(\sigma_u^2 + \sigma_v^2 + \sigma_w^2)$. Because canopy flows involve multiple length scales, the key ones are reviewed. The $L_c = (C_d a_s)^{-1}$ is the adjustment length scale[55,56] measuring how quickly the turbulent kinetic energy in eddies advecting at U is dissipated by their work to overcome the drag elements characterized by a drag coefficient C_d and leaf area density a_s, $\eta = (\nu^3/\varepsilon)^{1/4}$ is the Kolmogorov micro-scale with ε being the mean dissipation rate of K at z, and ν is the kinematic viscosity. The shear length scale, L_s, that measures the thickness of the vortical structures produced by Kelvin–Helmholtz instabilities and the length scale of attached eddies to the zero plane displacement, L_{BL}, are defined as

$$L_s = \frac{U_h}{\Gamma(h)}, \tag{3}$$

$$L_{BL} = \kappa_v(z - d) \tag{4}$$

with $U_h = U(h)$ being the mean velocity at $z/h = 1$.[3,35] It is to be noted that for dense canopies and under certain simplifying assumptions, d/h and L_s/h follow a complementary relation $[d + (1/2)L_s]/h = 1$.[4,28] Other complementary relations between d/h and L_s/h have also been proposed, most notably the expression $d/h + A_{sk}L_s/h = 1$, where A_{sk} was determined to be between 0.4 and 0.65 (instead of 0.5) using imbalances in production and destruction of K[24] with A_{sk} reduced with increasing K transport. To be clear, choices made about

d are not independent of L_s and may depend on the imbalances in the K budget. These imbalances are the main motivation for the introduction of the dissipation length scale

$$L_d = \frac{u_*^3}{\varepsilon(z)} \tag{5}$$

and has been used in roughness sublayer studies.[50–52] While L_d is labeled as a dissipation length scale, it is emphasized that L_d is an integral scale much larger than η. In fact, $L_d/\eta = (u_*/v_k)^3$, where $v_k = (\nu\varepsilon)^{1/4}$ is the Kolmogorov velocity satisfying $Re_k = v_k\eta/\nu = 1$, and Re_k is the micro-scale Reynolds number formed by the micro-scale turbulent diffusivity $v_k\eta$ and molecular viscosity ν. A macro-scale Reynolds number can then be defined as $Re_d = u_*L_d/\nu = (u_*/v_k)^4$. Hence, $L_d/\eta = Re_d^{3/4}$ and is consistent with the Reynolds number-dependent separation between macro- and micro-scales in many turbulent flows.[57] This estimate of $L_d/\eta = Re_d^{3/4}$ is independent of how ε is determined and emerges from definitions.

B. The inertial sublayer (ISL) region and the moving equilibrium hypothesis

Contrary to many agricultural sites, forests are rarely situated on uniform and flat terrain. A brief discussion on key restrictions to accommodate some aspects of these non-ideal effects within ϕ_{RSL} estimates is presented using the so-called moving-equilibrium hypothesis.[58] Three key budgets in the ISL for stationary and planar homogeneous high Re_d flow in the absence of subsidence are reviewed.

(i) The mean vertical momentum balance ($\partial\bar{w}/\partial t = 0$, t is time) that leads to an expression for $\sigma_w^2 = \overline{w'w'}$ is given by

$$\frac{\partial\overline{w'w'}}{\partial z} = -\frac{1}{\bar{\rho}}\frac{\partial\bar{P}}{\partial z} - g, \tag{6}$$

where P is the pressure and g is the gravitational acceleration. Clearly, mean hydrostatic conditions require that $\partial\sigma_w^2/\partial z = 0$ (expected in a near-neutrally stratified ISL).

(ii) The mean longitudinal momentum balance ($\partial U/\partial t = 0$) that leads to

$$\frac{\partial\overline{w'u'}}{\partial z} = -\frac{1}{\bar{\rho}}\frac{\partial\bar{P}}{\partial x}. \tag{7}$$

In the absence of a mean longitudinal pressure gradient, $\overline{u'w'} = -u_*^2$ and is independent of z. Its value may be set at $z/h = 1$. Measured deviations from a constant σ_w^2 and $\overline{u'w'}$ with z may signify modifications to $\bar{P}$ expected over non-flat terrain. Providing these modifications to $\bar{P}$ are not too large to introduce mean advective terms, the assumptions of stationary and planar homogeneous flow conditions in the absence of subsidence may still hold in the ISL though the independence of stresses and σ_w^2 from z may not. This is the essence of the moving equilibrium hypothesis,[58,59] which has been shown to collapse some similarity laws in the RSL over forests[60] and on complex terrain covered with forests for σ_w.[61]

(iii) The turbulent kinetic energy balance (i.e., $\partial K/\partial t$) in the absence of all transport terms (pressure and turbulence) can be reduced to

$$P_m = -\overline{u'w'}\Gamma(z) = \varepsilon, \qquad (8)$$

where P_m is the mechanical production of K. In the idealized ISL, $\varepsilon = P_m = u_*^2\Gamma$ and $\Gamma = (u_*/L_{BL})$. Only under those conditions is $L_d = L_{BL}$. A formal link between L_d, L_{BL}, and ϕ_{RSL} will be established later on using the simplified co-spectral budget model in which the shape of the vertical velocity spectrum is externally supplied. Thus, the work here contributes to the growing evidence that deviation of L_d/L_{BL} from unity is a key factor to explaining many features of the RSL[51,52] including ϕ_{RSL}.

C. Model 1: A stress budget model

In stationary and planar homogeneous high Reynolds number flow and in the absence of subsidence, the turbulent stress budget reduces to[40]

$$\frac{\partial \overline{w'u'}}{\partial t} = 0 = -\sigma_w^2\Gamma(z) - \frac{\partial \overline{w'w'u'}}{\partial z} + R_{u,w} - 2\varepsilon_{uw}, \qquad (9)$$

where the terms on the right-hand side, respectively, are the mechanical (or covariance) stress production, the flux transport, the pressure-rate-of-strain de-correlation ($R_{u,w}$), and the viscous de-correlation term (ε_{uw}). Upon ignoring the flux transport relative to the mechanical production and the viscous de-correlation term relative to $R_{u,w}$ (to be discussed later), and upon using a conventional Rotta return-to-isotropy closure scheme to represent $R_{u,w}$ corrected for the isotropization of the production, the turbulent stress budget reduces to

$$-(1 - C_I)\sigma_w^2\Gamma(z) - C_R\frac{\overline{w'u'}}{\tau} = 0, \qquad (10)$$

where $C_I = 3/5$ is a constant associated with the fast isotropization of the production term whose numerical value has been derived from rapid distortion theory,[40,53] $C_R = 1.8$ is the Rotta constant associated with the slow pressure-rate-of-strain part, and τ is a de-correlation time scale. The so-called LRR-IP model for $R_{u,w}$ (after Launder, Reece, and Rodi including the isotropization of the production) has been chosen because it reproduces the mean velocity and stresses in various types of shear flows.[40,62–65] Equation (10) can be written as

$$-\frac{1}{A}\frac{\tau\sigma_w^2}{\overline{w'u'}}\Gamma(z) = 1, \qquad (11)$$

where $A = C_R/(1 - C_I) = 4.5$. Comparing Eqs. (11) and (1) allows ϕ_{RSL} to be formulated as

$$\phi_{RSL} = -A\frac{\overline{u'w'}}{u_*^2}\frac{u_*}{\sigma_w}\frac{L_{BL}}{\tau\sigma_w}. \qquad (12)$$

Equation (12) suggests that the RSL introduces deviations from $\phi_{RSL} = 1$ through two key mechanisms: (i) an $\overline{u'w'}/u_*^2$ and σ_w/u_* dependency on z presumably due to the presence of complex topography distorting $\bar{P}$ from its idealized ISL budget expectations, and (ii) a $\tau\sigma_w$ that no longer scales with L_{BL}. This second dependency is more difficult to anticipate for the RSL as $\tau\sigma_w$ may be sensing multiple

length scales (e.g., L_{BL}, L_s, L_d, L_c, and η) that require spectral information to unpack them and frames the scope here. However, to offer foresight, an analogy to Lagrangian structure function analysis[40] is employed to formulate a plausible estimate of τ. In this analogy, it is assumed that the Lagrangian time scale and τ are proportional to each other and we select $\tau = 2\sigma_w^2/\varepsilon$ without any extra proportionality coefficient. This estimate of τ leads to

$$\phi_{RSL} = -\frac{A}{2}\frac{\overline{u'w'}}{u_*^2}\left(\frac{u_*}{\sigma_w}\right)^4\frac{L_{BL}}{L_d}. \qquad (13)$$

As a check to Eq. (13), the ISL is considered where $\overline{u'w'} = -u_*^2$, $\sigma_w/u_* = A_{ww} = 1.2$, $P_m = \varepsilon$ with $P_m = u_*^2\Gamma$, and $\Gamma = u_*/L_{BL}$ (i.e., law of the wall). Upon inserting all these estimates into Eq. (13) yields a $\phi_{RSL} = A/(2A_{ww}^4) = 1.08$, which is close to unity based on this selected choice of τ. Equation (13) can also be used to infer the thickness of the RSL by finding the z for which L_{BL}/L_d yields $\phi_{RSL} = 1$.

Equation (13) is now labeled as model 1 and will be used to estimate how ϕ_{RSL} deviates from unity as the canopy top is approached from the ISL with decreasing z/h. Model 1 sets the background for the second model for ϕ_{RSL} based on the co-spectral budget. Commencing with the normalizing property $\int_0^\infty E_{ww}(k)dk = \sigma_w^2$, where $E_{ww}(k)$ is the vertical velocity energy spectrum at wavenumber k along the x direction, the presence of an RSL is expected to distort $E_{ww}(k)$ from its "canonical" shape in the ISL. These distortions can then be translated to ϕ_{RSL} estimates at various z/h values, which can be achieved through a co-spectral budget (CSB) model described next (model 2). The basic properties of $E_{ww}(k)$ at production to inertial subrange (ISR) scales at various z/h have been studied and reviewed recently[42] making their connection to ϕ_{RSL} timely.

D. Model 2: The co-spectral budget (CSB) model

The momentum flux $\overline{w'u'}$ can be linked to eddy sizes or scales using the normalizing property

$$-\overline{w'u'} = \int_0^\infty F_{wu}(k)dk, \qquad (14)$$

where $F_{wu}(k)$ is the one-dimensional co-spectrum at wavenumber k also defined along the x direction. A CSB model, originally developed for locally homogeneous turbulence, is given as[66,67]

$$\frac{\partial F_{wu}(k)}{\partial t} + 2\nu k^2 F_{wu}(k) = P_{wu}(k) + T_{wu}(k) + \pi(k), \qquad (15)$$

where $\varepsilon_{wu} = 2\nu\int_0^\infty k^2 F_{wu}(k)dk$ is the viscous dissipation of the turbulent stress as before, $P_{wu}(k) = -\Gamma(z)E_{ww}(k)$ is the mechanical stress production term, $T_{wu}(k)$ is the co-spectral flux-transfer term across scales, and $\pi(k)$ is the velocity–pressure interaction term, related to the pressure-rate-of-strain R_{uw}. For stationary and planar homogeneous flows in the ISL, Eq. (15) reduces to

$$2\nu k^2 F_{wu}(k) \approx -\Gamma(z)E_{ww}(k) + \pi(k). \qquad (16)$$

Here, $T_{wu}(k)$ is ignored relative to $\pi(k)$ as shown from direct numerical simulations discussed elsewhere[66] and other scaling arguments.[53] To establish a relation between $\Gamma(z)$, $E_{ww}(k)$, and $F_{wu}(k)$ based on Eq. (15), a closure for the pressure–velocity co-spectrum $\pi(k)$ is again needed. A scale-wise closure for $\pi(k)$ with a scale-wise isotropization

of the production term that corrects the original Rotta scheme is used and is given by[40,64,68,69]

$$\pi(k) = C_R \frac{F_{wu}(k)}{\tau(k)} - C_I P_{wu}(k), \tag{17}$$

where $\tau(k)$ is now interpreted as a scale-dependent de-correlation time scale. Under this closure assumption, the CSB model for $F_{wu}(k)$ reduces to

$$(1 - C_I)\Gamma(z)E_{ww}(k) - \frac{C_R}{\tau(k)}F_{wu}(k) = 2\nu k^2 F_{wu}(k). \tag{18}$$

The relative importance of the Rotta (or slow) component and the viscous dissipation term is given as[53]

$$\frac{2\nu k^2 F_{wu}(k)}{C_R F_{wu}(k)/\tau(k)} = \frac{2}{C_R}\left(\frac{\nu^3 k^4}{\varepsilon}\right)^{1/3} = \frac{2}{C_R}(k\eta)^{4/3}. \tag{19}$$

Noting that $C_R = 1.8$ and for $k\eta \ll 1$, the de-correlation due to viscous effects can be ignored relative to the Rotta term (as assumed in the stress budget earlier). As $k\eta \to 1$, these two de-correlation terms become comparable in magnitude though their combined contributions to the overall $\overline{w'u'}$ is negligible at those locally isotropic scales. Hence, for analytical tractability, the viscous de-correlation term is ignored throughout at all k relative to $\pi(k)$. With these simplifications and closure assumptions for $\pi(k)$,

$$-F_{wu}(k) = A^{-1}\Gamma(z)\tau(k)E_{ww}(k), \tag{20}$$

where $\tau(k) = \alpha\varepsilon^{-1/3}k^{-2/3}$ is the relaxation time at k associated with turbulent stress de-correlation,[53,54,66,70] and α is a proportionality constant of order unity. Upon integrating Eq. (20), a spectral version of Eq. (12) is obtained so that ϕ_{RSL} can be expressed as

$$\phi_{RSL} = -A\left(\frac{\overline{u'w'}}{u_*^2}\right)\left(\frac{u_* L_{BL}}{\int_0^\infty \tau(k)E_{ww}(k)dk}\right). \tag{21}$$

Distortions to the scale-wise product $\tau(k)E_{ww}(k)$ by the RSL away from their canonical ISL shapes can now be directly linked to deviations of ϕ_{RSL} from unity. Equation (21) is labeled as model 2 when the measured $E_{ww}(k)$ is used at each z/h to evaluate ϕ_{RSL}.

Before proceeding to a simplified version of model 2, a comment about ignoring $T_{wu}(k)$ in the RSL is in order given that L_{BL} may be small in the RSL. Specifically, it has been shown that in the presence of strong shear, $T_{wu}(k)$ can be ignored for $kL_{co} \gg 1$, where $L_{co} = \sqrt{\varepsilon/\Gamma^3}$ is the Corrsin scale.[71,72] In the ISL where $P_m = \varepsilon$ and Γ is given by the law of the wall, $L_{co} = L_{BL}$. High Reynolds number canonical boundary layer experiments already demonstrated an onset of $F_{wu}(k) \sim \Gamma k^{-7/3}$ [i.e., ignoring $T_{wu}(k)$] for $kL_{BL} > 1$ instead of $kL_{BL} \gg 1$.[72] Moreover, these same experiments show that the onset of a $k^{-7/3}$ scaling in the co-spectrum occurs at eddy sizes larger than those at which the $k^{-5/3}$ commences in the much studied inertial subrange region (ISR) of $E_{ww}(k)$. Several conjectures have been offered and are reviewed elsewhere[70] as to why. These studies show that $\tau(k)$ and $E_{ww}(k)$ adjust to maintain a $k^{-7/3}$ in the co-spectrum while preserving linearity between $F_{uw}(k)$ and Γ. Returning to the RSL, L_{co} can be related to L_{BL} and L_d from definitions using $L_{co} = \phi_{RSL}^{-1/2}\sqrt{L_{BL}^3/L_d}$. Compared to the ISL, $L_{co}/L_{BL} = \phi_{RSL}^{-1/2}\sqrt{L_{BL}/L_d}$. While $L_{BL}/L_d < 1$

in the RSL is to be expected, this reduction is more than compensated for by $\phi_{RSL} < 1$. Hence, in the ISR, $F_{wu}(k) \sim \Gamma k^{-7/3}$ still holds for $kL_d > 1$ as will be demonstrated later on for the experiments here.

E. Model 3: A simplified co-spectral budget (CSB) model

As earlier noted, to model ϕ_{RSL} using Eq. (21), it requires $E_{ww}(k)$. An ideal shape for $E_{ww}(k)$ is introduced so as to arrive at a closed-form expression that links ϕ_{RSL} to L_d while accommodating all the energetics of the flow albeit via an assumed $E_{ww}(k)$. We label this outcome as model 3. The rationale behind this simplified treatment is that virtually all experiments in the RSL, including measurements conducted at $z/h = 1$, confirm the presence of an extensive ISR in $E_{ww}(k)$ at $kh > 1$.[42,54,73] Thus, an ISR is expected at high wavenumbers (but for $k\eta \ll 1$) where $E_{ww}(k) \sim k^{-5/3}$. At large scales, the $E_{ww}(k)$ may be characterized by an energy-splashing region [i.e., $E_{ww}(k) \sim k^0$]. A model of maximum simplicity is to introduce a transition wavenumber between them designated by k_a (to be discussed later on). These two limiting regimes have received numerous experimental support for near-neutral stratification and close to the ground.[42,69,74,75] This model for $E_{ww}(k)$ ensures continuity but not smoothness at k_a and is thus given as

$$E_{ww}(k) = C_o\varepsilon^{2/3}k_a^{-5/3} \quad \forall \ k/k_a \leq 1, \tag{22}$$
$$E_{ww}(k) = C_o\varepsilon^{2/3}k^{-5/3}, \quad \forall \ k/k_a > 1, \tag{23}$$

where $C_o = (24/55)C_e$ is the Kolmogorov constant for the one-dimensional vertical velocity energy spectrum, and $C_e = 1.5$ is the Kolmogorov constant for the turbulent kinetic energy spectrum.[40] With this representation, k_a and ε are the only two unknowns that completely specify $E_{ww}(k)$. Moreover, imposing the normalization condition $\int_0^\infty E_{ww}(k)dk = \sigma_w^2$ requires that

$$\frac{1}{k_a L_d} = \left[\left(\frac{2}{5C_o}\right)^{1/2}\left(\frac{\sigma_w}{u_*}\right)\right]^3. \tag{24}$$

When inserting the assumed $E_{ww}(k)$ [Eqs. (22) and (23)] and $\tau(k)$ into Eq. (21) and enforcing the outcome of Eq. (24) yields

$$\phi_{RSL} = -\frac{5}{3}\frac{AC_o}{\alpha}\left(\frac{\overline{u'w'}}{u_*^2}\right)\left(\frac{u_*}{\sigma_w}\right)^4\frac{L_{BL}}{L_d}. \tag{25}$$

Equation (25), which is labeled as model 3, underscores the link between ϕ_{RSL} and L_{BL}/L_d arising from $E_{ww}(k)$ already derived in Eq. (13). As before, a lack of equilibrium in the K budget (i.e., $P_m/\varepsilon \neq 1$) can impact ϕ_{RSL} through L_d. The normalizing condition on $E_{ww}(k)$ also suggests that $k_a \propto 1/L_d$ with a proportionality coefficient that depends on $(\sigma_w/u_*)^3$. Last, Eqs. (25) and (13) become identical when setting $\alpha = 10C_o/3$ in the formulation of $\tau(k)$. The three models derived here will be compared to the ϕ_{RSL} directly estimated from Eq. (1) using multi-level velocity time series measurements from the ATTO research station and the GoAmazon site. It is to be noted that all three models derived here do not require d in their formulation of eddy-diffusivity. The emergence of d in the three models of ϕ_{RSL} is only due to L_{BL} being set as the basic length scale in the ISL.

III. DATASET DESCRIPTION

The data used were collected at two sites in Amazonia: the ATTO research station during the first intensive observation period (IOP-1) and the GoAmazon site during another intensive field campaign. The ATTO research station is located on a plateau approximately 130 m a.g.l. in a terra firma forest region, located 150 km in a straight line from the city of Manaus (Brazil). The velocity measurements were performed in the dry season from 25 October to 25 November 2015. However, all sonic anemometers only performed simultaneous measurements from the 11th to the 29th of November. During this period, the average canopy height of the surrounding forest was 37 m, which is set to h. The leaf area index (LAI) in the vicinity of the tower is about 5.5–7.5 m^2 m^{-2} as discussed elsewhere.[48,76] Assuming a typical $C_d = 0.2$ and a leaf area density $a_s = LAI/h$ yields an L_c/h that is roughly of order unity. A $d/h = 0.9$ was earlier estimated[45] and compared to other independent methods and literature values for dense canopies. This d/h value is adopted unless otherwise stated. Its consequences on ϕ_{RSL} are discussed later on. The three wind velocity components were measured at three heights: 40, 55, and 81 (a.g.l.) on an 80-m scaffolding tower (2°08.647′ S 58°59.992′ W.). The IOP-1 also included measurements at 150 (a.g.l.) on a 325-m steel lattice tower (2°08.752′ S 59°00.335′ W.). The two towers are separated by 670 m.[45] Because this separation distance and near-neutral stratifications were rarely recorded at this elevation, the data from this sonic anemometer were not employed. At heights 40 and 55 m, measurements were performed by CSAT3, Campbell Scientific, Inc., sonic anemometers, while at 81 m a Windmaster, Gill Instruments Limited, sonic anemometer was installed. All sonic anemometers were sampled at a frequency $f_s = 10$ Hz and the raw data stored for future processing. Detailed description of the ATTO site and the (IOP-I) measurement campaign is presented elsewhere[1,45] and is not repeated here.

The GoAmazon data were collected at a 50-m tall tower (2°36.5′ S 58°12.5′ W.) located at 130 m a.g.l (known as K34) some 60 km north–northwest of Manaus. The site is on top of a plateau surrounded by a dense primary forest with characteristics similar to the ATTO site. The mean canopy height was $h = 35$ m and LAI $= 6$ m^2 m^{-2}. All velocity components above the canopy were measured using three triaxial sonic anemometers (model CSAT3, Campbell Scientific, Inc., Logan, UT) set at $z/h = 1$, 1.15, and 1.38 commencing from 23 March 2014 to 16 January 2015. The sampling frequency was set to 20 Hz. Detailed description of the experimental field campaign is presented elsewhere.[77,78] Thus, the GoAmazon offers higher vertical resolution of the flow statistics in the RSL near the canopy top, whereas the ATTO site is focused on transitions between the RSL and ASL. Double rotations were used at all heights to ensure that $\bar{w} = \bar{v} = 0$. The analysis resulted in seven 1-h runs for the ATTO and 25 1-h runs for the GoAmazon that are stationary with mean wind directions that are consistent across all z. The friction velocity at the canopy top was estimated from $u_* = (|\overline{w'u'}|^2 + |\overline{w'v'}|^2)^{1/4}$. Longitudinal [$E_{uu}(f)$] and vertical [$E_{ww}(f)$] velocity spectra as a function of frequency (f) were evaluated using fast Fourier transforms. Different from several prior studies[42,79] that used 30-min subsets, the present analysis employs 1-h runs to resolve low-frequency influences on the spectral scaling exponents.

For the ATTO data, the $\varepsilon(z)$ values were computed from the longitudinal velocity spectrum $E_{uu}(k)$ in the ISR using Taylor's frozen turbulence hypothesis to convert f to k, where the wavenumber

$k = 2\pi f/U$. Although the turbulent intensity in the RSL is large, the validity of Taylor's hypothesis remains acceptable as discussed elsewhere.[42,80] A comparison between ε estimated from the ISR of $E_{uu}(k)$ and $E_{ww}(k)$ was also conducted for the ATTO data and the difference between them was found to be under 10 % when all runs and z values were considered. For the GoAmazon data, $\varepsilon(z)$ values were calculated from the longitudinal velocity second-order structure functions using the slope of the structure function in the ISR and are already discussed elsewhere.[50] The rationale for using the longitudinal velocity spectrum or structure function were twofold: (i) $\varepsilon(z)$ is determined independent from $E_{ww}(k)$, and (ii) the ISR spans more scales for the longitudinal velocity spectra and structure functions compared to their vertical velocity counterparts, thus yielding robust estimates of the dissipation rate. The $\Gamma(z)$ was estimated after fitting a third-order polynomial in $\log(z)$ to U and computing derivatives analytically from fitted coefficients.

The transition wavenumbers k_a were estimated from the maxima of the average pre-multiplied spectra $kE_{ww}(k)$ (Fig. 4). Two methods were used: (i) evaluating the maximum of a spline interpolation of the averaged pre-multiplied spectra and (ii) fitting each 1-h sampled pre-multiplied spectra with generic forms[37] as discussed elsewhere.[42] This form is given as $0.164(k/k_0)/[1 + 0.164(k/k_0)^{5/3}]$ and leads to $k_a = 3.77k_0$, where k_0 is determined from fitting to measured pre-multiplied spectra. Since no appreciable difference was found between the two methods, the k_a results derived from the second method are shown for consistency with prior results.[42]

Only data collected in near-neutrally stratified atmospheric conditions were considered in the analysis. 7 and 25 h were, respectively, used for the ATTO and the GoAmazon data sets.

IV. RESULTS

To address the two questions, Sec. IV is organized as follows. The height dependence of the main bulk flow statistics relevant to the CSB model prediction of ϕ_{RSL} (primarily $\overline{u'w'}/u_*^2$, σ_w/u_*, and P_m/ε) is first discussed. Next, the spectra and co-spectra as well as the predictions of $F_{uw}(k)$ from $E_{ww}(k)$ using the CSB model are presented. Since the CSB model assumes that $\tau(k) = \alpha\varepsilon^{-1/3}k^{-2/3}$, an investigation of this assumption for the various k along with the optimal α is considered. One of the key findings from the CSB model with an idealized $E_{ww}(k)$ representation is that k_aL_d must be constant when $E_{ww}(k)$ is normalized by σ_w^2. This finding is explored along with other possible scaling variables for k_a. Last, predictions of ϕ_{RSL} from the proposed formulations are compared.

A. Bulk flow statistics

Figure 1 presents U/u_*, σ_w/u_*, $\overline{u'w'}/u_*^2$, and P_m/ε as a function of normalized height z/h, where u_* is defined at the canopy top at both sites. The extrapolated values of $U/u_* = 3.3$ to the canopy top are commensurate with typical values ($U_h/u_* \sim 3.3$) reported for dense canopies in field experiments, wind tunnels, and flumes[3,26,35] for both data sets. The σ_w/u_* near the canopy top is higher than expectations from mixing layer (ML) analogy arguments (=1.15) for ATTO but consistent with the ML analogy for the GoAmazon. Further away from the canopy top ($z/h > 2$), σ_w/u_* is near unity instead of its expected near-neutrally stratified surface layer value (i.e., $A_w = 1.2 - 1.3$) for ATTO. These average patterns of σ_w/u_* are consistent with prior studies[45–47] at ATTO and reflect the behavior of the
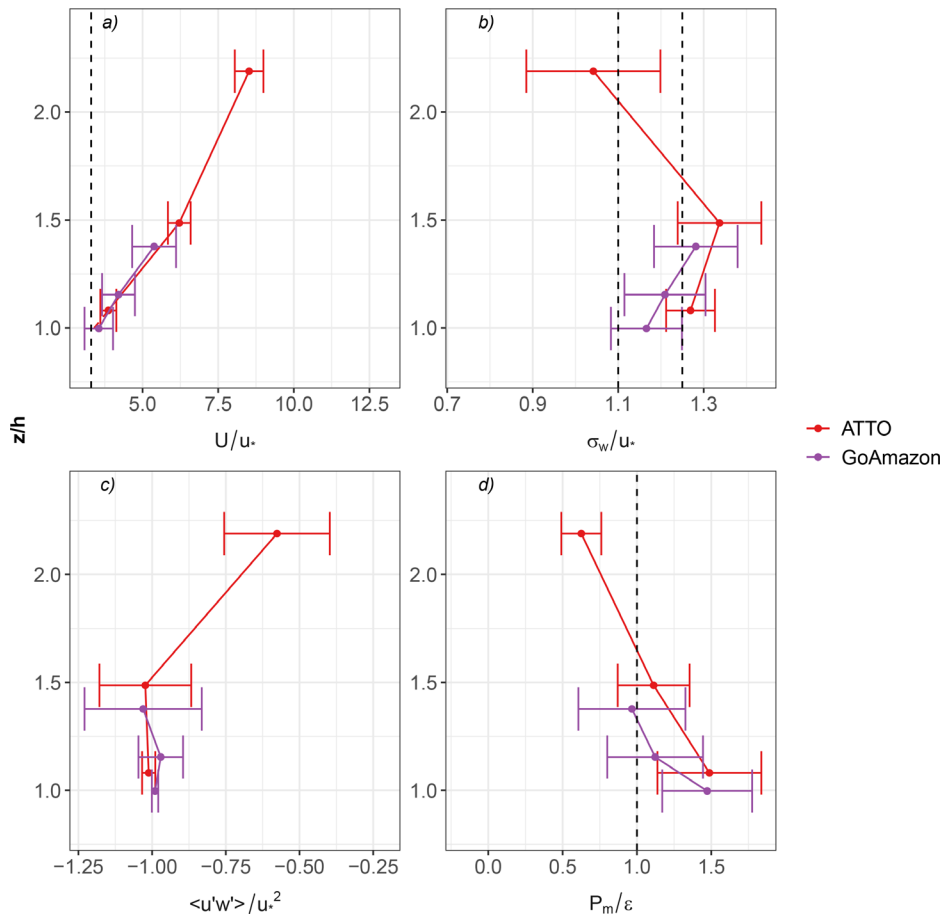
FIG. 1. Profiles of U/u_* [panel (a)], σ_w/u_* [panel (b)], $\overline{u'w'}/u_*^2$ [panel (c)], and P_m/ε [panel (d)] as a function of normalized height z/h for ATTO and GoAmazon. The dashed lines refer to: in panel (a) the 3.3 reference value for dense canopy; in panel (b) to the reference mixing layer, 1.1, and near neutral surface layer, 1.25, values; in panel (d) to the perfect balance between production and dissipation.

individual profiles (not shown). More crucial is that σ_w/u_* is not independent of z for both sites. Likewise, the turbulent stress $\overline{w'u'}/u_*^2$ profile is clearly not constant with z at both sites. That $\overline{w'u'}/u_*^2$ and σ_w/u_* are varying with z and are both suggestive that topographic effects are impacting $\bar{P}$. The data here broadly suggest that as z/h increases, $-\overline{u'w'}/u_*^2$ decreases but $(u_*/\sigma_w)^4$ increases. Since ϕ_{RSL} scales with both $-\overline{u'w'}/u_*^2$ (decreasing with z/h) and $(u_*/\sigma_w)^4$ (increasing with z/h), the product $-\overline{u'w'}/u_*^2$ and u_*/σ_w might partly compensate each other in the ϕ_{RSL} determination at GoAmazon and to a lesser extent ATTO. This finding underscores the significant role of L_{BL}/L_d in shaping the z variations in ϕ_{RSL}. The key quantity impacting L_{BL}/L_d is P_m/ε. In the neutral atmospheric surface layer (or ISL), there is ample experimental support for $P_m/\varepsilon = 1$.[51,72,81–83] However, numerous experiments and direct numerical simulations have already demonstrated that P_m/ε can be as large as 2 near the canopy top for neutral conditions,[51,82,84] and a value commensurate to P_m/ε reported in the buffer layer below the ISL of smooth-wall boundary layers.[40] The experiments here suggest that P_m/ε is indeed large and exceeds 1.5 near the canopy but drops below unity for $z/h > 1.3$ instead of attaining a unity value as expected in the ISL. For GoAmazon, this drop may be due to the rapid decline $-(\overline{u'w'}/u_*^2)$ with increasing z as $P_m/\varepsilon = (\overline{u'w'}/u_*^2)(L_{BL}/L_d)$. That is, the measured drop in $-\overline{u'w'}/u_*^2$ at both sites is large compared to previous

RSL experiments reported elsewhere[3] for $z/h = 1$ and $z/h = 2.2$. Previous work has attributed this drop in P_m/ε below unit to the effects of the topography at both sites.[48,85] Both observations[48] and large-eddy simulation (LES)[85] showed that the presence of even a gentle topography modifies the turbulent kinetic energy budget, producing complex profiles that do not conform with canonical surface layer scaling. Hence, the departure of the profiles in Fig. 1 depends on both the presence of a RSL and on topography.

B. Spectral and co-spectral properties

The measured averaged spectral and co-spectral shapes at all levels are featured in Fig. 2 at both sites. From this figure, it can be seen that measured $E_{uu}(k)$ exhibits an extended ISR (i.e., $k^{-5/3}$) scaling at all levels for smaller eddies ($kz > 1$), including z/h near unity consistent with numerous experiments and simulations.[42,73] However, as z/h increases and presumably the influence of RSL turbulence weakens, the onset of a k^{-1} scaling becomes evident at low wavenumbers ($kz < 1$) suggestive of dominance of attached eddies.[42,86–88] The $E_{ww}(k)$ also exhibits an extended ISR scaling for $kz > 1$ at all z. However, at $kz < 1$, the emerging picture is rather different. Near the canopy top, the measured $E_{ww}(k)$ is well approximated by the idealized shape assumed in Eq. (22). This finding is underscored by the
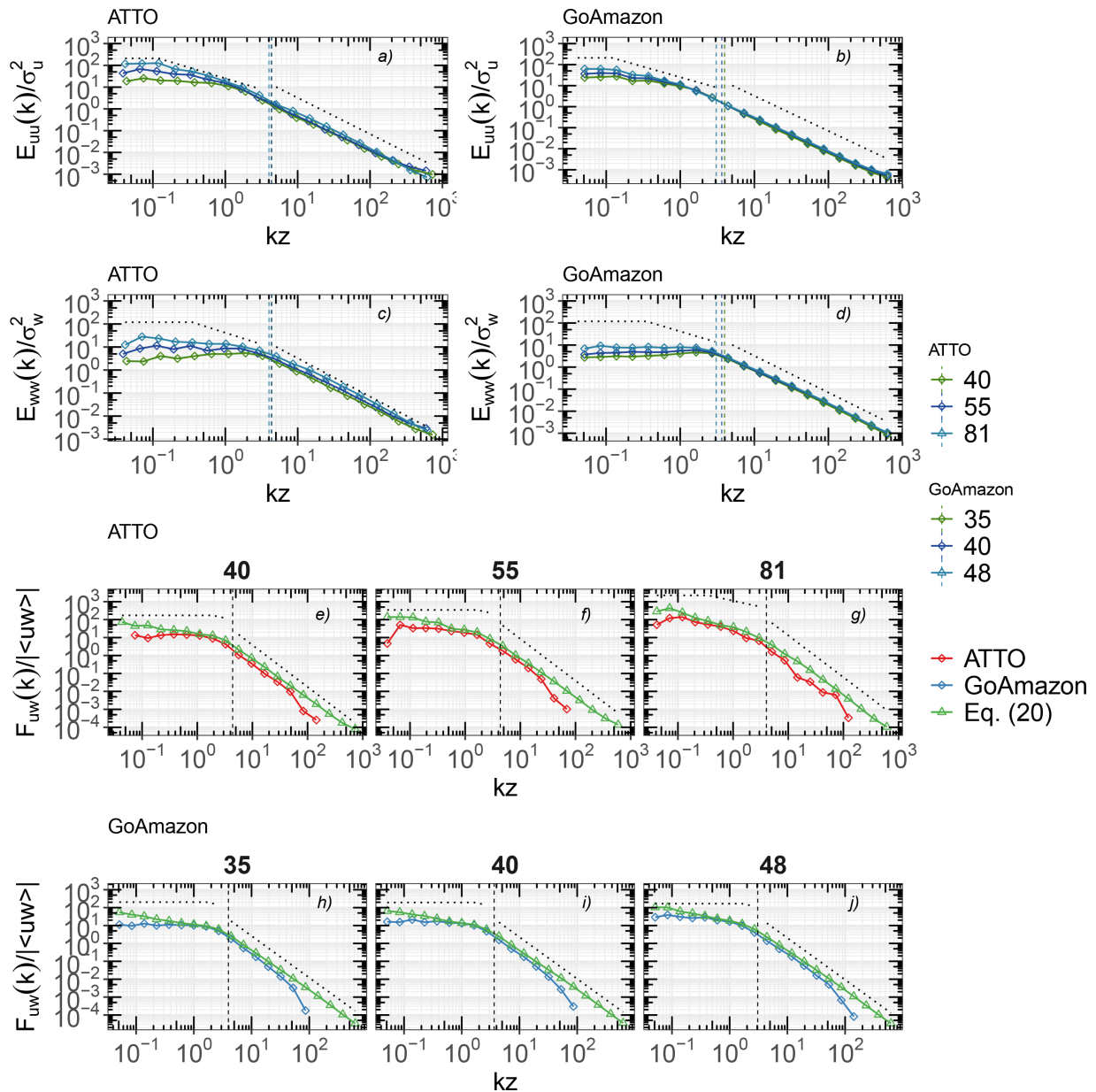
FIG. 2. Measured longitudinal velocity spectra $E_{uu}(k)/\sigma_u^2$ (top row), vertical velocity spectra $E_{ww}(k)/\sigma_w^2$ (middle row), and co-spectra $F_{uw}(k)/|\overline{u'w'}|$ (bottom two rows) for ATTO and GoAmazon. For the co-spectra, the columns represent the three heights (increasing from left to right). The vertical dashed line is $k_a z = 1$. The expected scaling exponents k^0, $k^{-2/3}$, k^{-1}, $k^{-5/3}$, and $k^{-7/3}$ are also featured as dotted lines in their respective subranges (i.e., k^0 for energy-splashing range, k^{-1} for attached eddy range, and $k^{-5/3}$ for ISR in the energy spectra, and k^0 or $k^{-2/3}$ and $k^{-7/3}$ in the ISR for the co-spectra). The predicted co-spectra from Eq. (20) using $\alpha = 10C_o/3$ and measured Γ in Fig. 1) and measured $E_{ww}(k)$ (middle row) are also shown in the bottom row.

GoAmazon data that interrogates the near canopy top region $z/h \in [1, 1.3]$ better than ATTO. With increasing z/h, deviations from a "flat" or "energy-splashing" (i.e., k^0) region at $kz < 1$ become noticeable but small. Increasing z/h, $E_{ww}(k)$ exhibits a scaling exponent $k^{-\beta}$ with β increasing from 0 (near $z/h = 1$) to a small but finite (sub-unity) value (for $z/h \sim 2.2$). This increase was also documented in a number of field experiments reviewed elsewhere.[42] The reason for this

increase is dynamically interesting and is the subject of a future study. It suffices to note that earlier studies argued that a k^{-1} scaling should exist in $E_{ww}(k)$ at $kz < 1$ for near-neutrally stratified boundary layers in the ISL[89] and other wall-bounded flows.[90] However, this scaling remains difficult to ascertain given its restricted range and controversy surrounding it. Nonetheless, what is not in dispute is that deviations from k^0 in $E_{ww}(k)$ at $kz < 1$ are present and their signatures in ϕ_{RSL}

can be explored using the CSB model (model 2). How well the CSB model performs is diagnosed in Fig. 2 [panels (i), (j), and (k)] by comparing the predicted $F_{uw}(k)$ from Eq. (20) with measured $F_{uw}(k)$ for all k using $\alpha = 10C_o/3$. Both measurements and predictions at all z agree to the onset of a $k^{-7/3}$ scaling at $kz > 1$ (i.e., the ISR with finite Γ). However, due to measurement limitations (random noise and path-averaging) at the highest k, a rapid decline in $F_{uw}(k)$ is noted in the experiments. These effects are expected to impact $F_{uw}(k)$ far more than $E_{ww}(k)$. The notable difference between measured and modeled $F_{uw}(k)$ is at $kz \ll 1$. Because $\tau(k) = \alpha\varepsilon^{-1/3}k^{-2/3}$, a $k^{-2/3}$ scaling is expected in modeled $F_{uw}(k)$ when $E_{ww}(k)$ experiences an energy splashing (or k^0) regime. However, the measured $F_{uw}(k)$ does not support a $k^{-2/3}$ scaling near the canopy top at $kz < 1$. Nonetheless, with increasing z/h, the measured and predicted $F_{uw}(k)$ do agree better at the low wavenumber end. Notwithstanding this issue at low k, the overall agreement between measured and modeled $F_{uw}(k)$ from Eq. (20) can be deemed acceptable for linking ϕ_{RSL} to $E_{ww}(k)$ at both sites. We recall that ϕ_{RSL} is sensitive to $\int_0^\infty \tau(k)E_{ww}(k)dk$ as in Eq. (21).

A comparison between measured and modeled averaged $\tau(k)$ as well as averaged α are presented in Fig. 3 for ATTO as the height variations are more substantial than the GoAmazon site. The "measured" averaged $\tau(k)$ and α are determined using Eq. (20) from measured Γ,

estimated ε, $F_{uw}(k)$, and $E_{ww}(k)$ at each height and for each hour and then averaging over all hours. The comparison here is suggestive that $\tau(k)$ is reasonably reproduced for $kz > 1$ at all z values as assumed in the analysis of the CSB [i.e., $\tau(k)$ scales as $k^{-2/3}$]. However, for $kz \ll 1$ and $z/h < 2$, $\tau(k)$ is becoming independent of k [i.e., measured $\tau(k)$ is approaching a k^0 instead of $k^{-2/3}$ for $z/h \rightarrow 1$]. This independence at $kz \ll 1$ from k may be hinting that canopy-scale processes are restricting τ at large scales (at least for $z/h = 1$). Clearly, these restrictions become weaker with increasing z/h. Figures 3(d)–3(f) show the limiting values of α: $\alpha = 1$ (blue line) and $\alpha = \frac{10}{3}C_o$ (green line), together with the value, $\bar{\alpha}$ averaged over all wavenumbers (purple). The influence of the limiting value of α on ϕ_{RSL} will be discussed further on.

C. Spectral peaks and the dissipation length scale

The agreement between measured and modeled $F_{uw}(k)$ prompted further investigation into the relation between measured k_a and L_d. Figure 4 shows the normalized pre-multiplied energy spectrum $kE_{ww}(k)/\sigma_w^2$ as a function of k along with different normalizations for k (abscissa): z, L_{BL}, L_S, and L_d. Again, the ATTO site is used for illustration given the wider coverage in z/h values. At all z/h, the
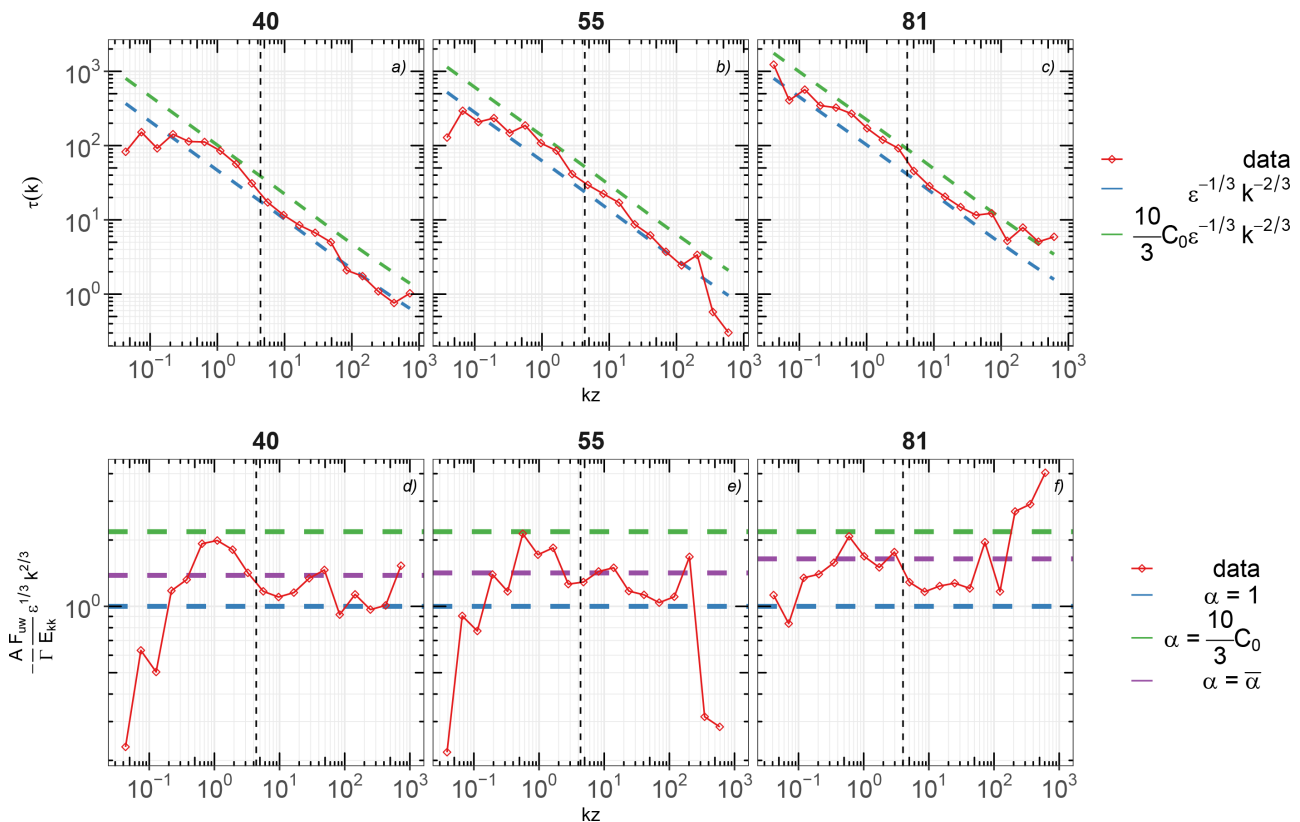
FIG. 3. Top panels: Comparison between measured (shown for ATTO for reference) and modeled de-correlation time scale $\tau(k)$ as a function of k at each measurement height z [panels (a)–(c)]. The red line refers to $\tau(k)$ estimated from Eq. (20). The blue and green lines refer to $\tau(k)$ estimated as $\alpha\varepsilon^{-1/3}k^{2/3}$ with $\alpha = 1$ and $\alpha = (10/3)C_o$, respectively. The dashed vertical line represents $k = k_a$. Bottom panels: Proportionality constant α of the modeled de-correlation time scale $\tau(k)$ from Eq. (20) as a function of normalized wavenumber kz at each measurement height z [panels (d)–(f)]. The red line refers to α estimated from Eq. (20). Horizontal lines identify a perfect $\varepsilon^{1/3}k^{-2/3}$ scaling with constant α ($\alpha = 1$ blue line, $\alpha = (10/3)C_o$ green line, $\alpha = \bar{\alpha}$ purple line) is the scale-wise average value of α.
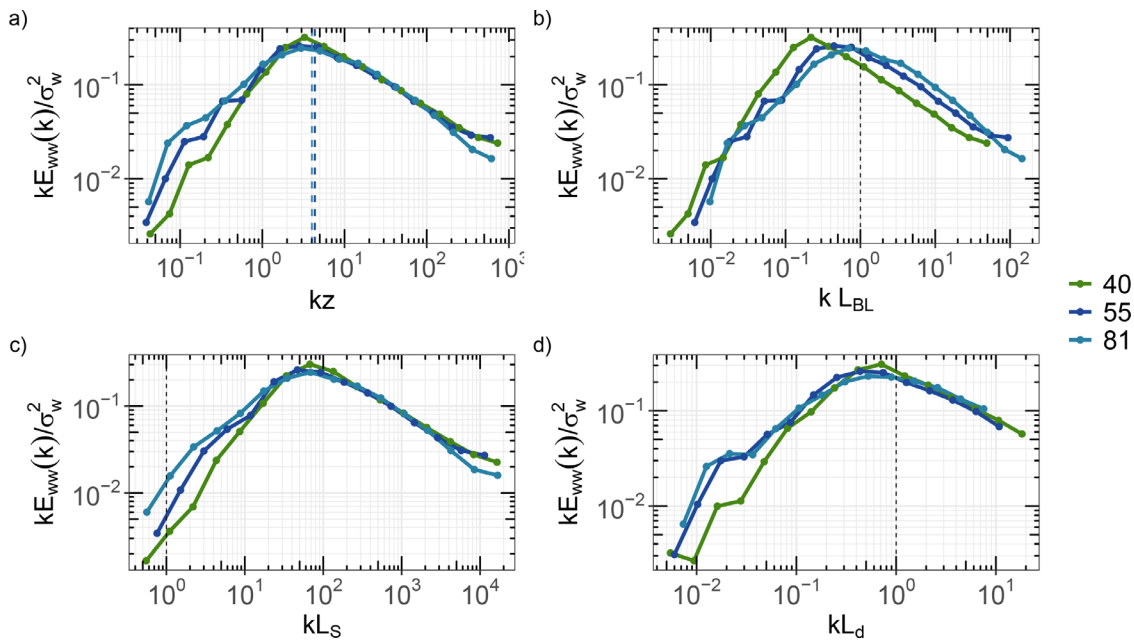
FIG. 4. Pre-multiplied normalized vertical velocity spectra, $k\,E_{ww}(k)/\sigma_w^2$ at different heights for ATTO as reference. Panel (a) shows the spectra as a function of $k\,z$. Panels (b), (c), and (d), represent k normalized using $k\,L[BL]$, $k\,L_s$ and $k\,L_d$, respectively. The vertical dashed lines refer to: in panel (a), k_a estimates at the different heights; in panels (b)–(d), $kL_\chi = 1$, where $L_\chi = L_{BL}$, L_s, and L_d. Note the collapse of the spectral peaks at $kL_d = 1$ for all z/h in panel (d).

pre-multiplied spectrum confirms that $0 \leq \beta < 1$, and thus, a k_a can be reasonably identified from the maximum of $kE_{ww}(k)/\sigma_w^2$. When normalizing k with L_{BL}, the peak location is not constant and varies with measurement height. The $kE_{ww}(k)/\sigma_w^2$ spectral peaks collapse to a single value when normalized by L_s, L_d, and z. However, the peaks associated with the L_s and z scaling are one to two orders of magnitude smaller in size (or larger in wavenumbers) than z or L_s. Interestingly, when L_d is used to normalize k, the peaks roughly align in the vicinity of $kL_d = 1$. This analysis provides experimental support to the finding from Eq. (24) that k_aL_d may be constant of order unity when the σ_w differences across z/h are accounted for through the normalization of the pre-multiplied energy spectrum here.

The profiles of inferred k_a from the spectral peaks in the pre-multiplied spectra and L_d are now shown in Fig. 5 at all levels and for the two sites. For reference, L_{BL} is also shown. All these length scales are normalized by the shear length scale (L_s) chosen because it does not vary with z/h. When using near-neutral stratification runs at ATTO, $L_s/h = 0.48$ is a representative mean value. Interestingly, for $z/h < 1.5$ all length scales ($1/k_a$, L_{BL}, and L_d) appear smaller in size when compared to L_s. For $z/h > 2$, both L_d and L_{BL} become sufficiently developed to exceed L_s. As expected, extrapolating L_{BL} to $z/h = 1$ produces length scales that are smaller than $1/k_a$, L_d, and L_s, meaning that attached eddies are not likely to be responsible for large momentum transport. Around $z/h = 1.5$, $1/k_a$, L_d, and L_{LB} are approximately equal. Predictions of Eq. (24) are also compared to measure k_aL_d in Fig. 5 for both sites. This comparison suggests that the link between k_a and L_d primarily depends on $(\sigma_w/u_*)^3$ variations with z though some unexplained variations around this constant are also noted albeit with uncertainty (see right panel).

D. Comparisons of ϕ_{RSL} model predictions

Having discussed all the three model assumptions, the ϕ_{RSL} profiles evaluated using Eq. (1), [Eq. (13), labeled as empirical in panel (a) or (25) with $\alpha = 10C_o/3$ [models 1 and 3 in panel (b)], and Eq. (21) for two values of α [model 2 in panels (c) and (d)] are compared in Fig. 6 for both sites. For reference, predictions from Eq. (2) with $a = 2$ and $a = 3$ and $z_*/h = 1.5$ and $z_*/h = 3$ are featured as those values encompass much of the literature ϕ_{RSL} ranges.[4] Based on Eq. (1), which may be treated as one possible definition of ϕ_{RSL}, a $\phi_{RSL} \to 1$ is attained around $z/h = 1.5$ and maintains its near-unity value for $z/h = 2.25$. Near the canopy top, $\phi_{RSL} < 1$ in agreement with logical expectations though its value remains larger than those predicted from Eq. (2) when using commonly reported z_* and a. Interestingly, Eq. (25) yields values commensurate with Eq. (2) when setting $z_*/h = 1.5$ and $a = 3$. Equation (21) leads to a $\phi_{RSL} < 1$ for all z/h when setting $\alpha = 10C_o/3 = 2.2$. Figure 6(d) suggests that α is a scaling parameter with $\phi_{RSL} \sim \alpha^{-1}$. Hence, setting $\alpha = 1$ would increase the computed ϕ_{RSL} curve by a factor of 2.2, thereby making the CSB-modeled ϕ_{RSL} much closer to Eq. (1) as shown in Fig. 6. Variations in α reflect how C_R is actually defined and may also be treated as deviations from its accepted 1.8 value (that is assumed here when determining A).

V. DISCUSSION

Having compared all three models with ϕ_{RSL} from Eq. (1), a discussion on the causes of the height dependence of ϕ_{RSL} and deviations between the models and empirical estimates from Eq. (1) is presented. As earlier mentioned, Eq. (1) requires an estimate of d and choices made about d may even "flip" $\phi_{RSL} < 1$ to $\phi_{RSL} > 1$. In all cases, L_{BL}/L_d, σ_w/u_*, and $\overline{u'w'}/u_*^2$ vary with z/h. These variations will be
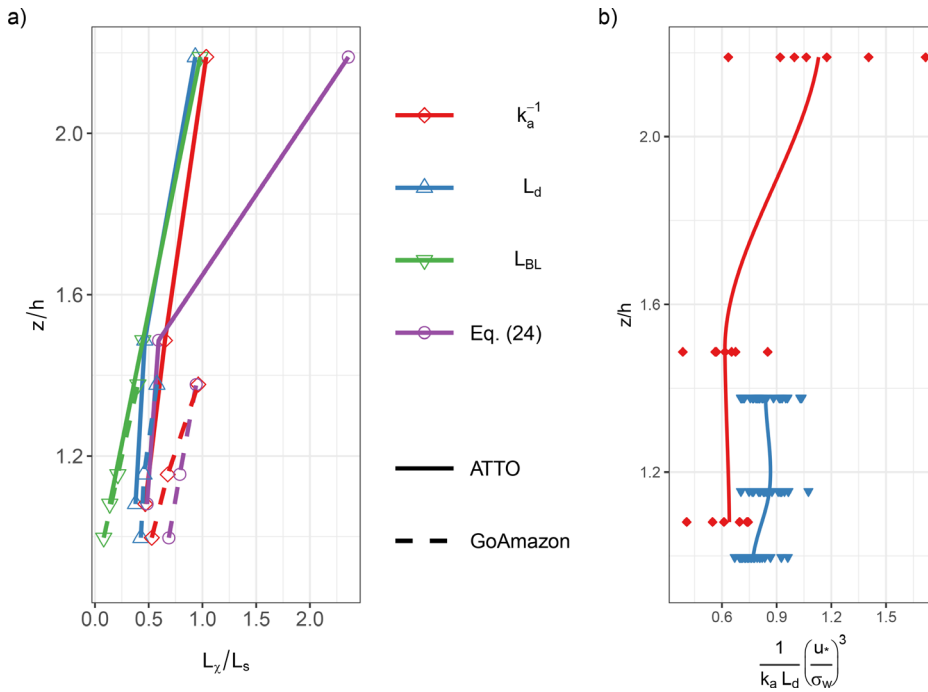
FIG. 5. Panel (a): Profiles of k_a^{-1} (red), L_d (blue), and L_{BL} (green) as a function of normalized height z/h for ATTO (continuous lines) and GoAmazon (dashed lines). The dashed red line represents L_d evaluated from Eq. (24). Panel (b): Comparison between $(k_a L_d)^{-1}(u_*/\sigma_w)^3$, red points. The continuous lines represent a local regression (LOESS) of the experimental points.

discussed here within the context of the validity of the moving-equilibrium hypothesis. Moreover, the $E_{ww}(k)$ shape was shown to vary with z/h at low wavenumbers, which impacts ϕ_{RSL} (as in model 2).

A. The moving equilibrium hypothesis

The RSL modifications to the law of the wall were considered within the context of the moving equilibrium hypothesis.[58] In this hypothesis, the mean pressure is allowed to gradually vary in x and z so that turbulent stresses and σ_w can also vary in x and z. The standard definitions of ϕ_{RSL} such as the one in Eq. (1) are now difficult to interpret because the mean momentum fluxes evolve in x and z. However, when $\bar{P}$ variations in x as well as deviations from hydrostatic conditions in z are assumed to be not too large to result in advective acceleration terms in the respective mean momentum balances, simplifications can be introduced to explain ϕ_{RSL}. The most significant simplification is that at a given x, the u_* at the canopy top becomes a local variable reflecting the overall local balance between friction (or canopy drag), variations in $\bar{P}$ (due to topography), and geostrophic winds. Thus, the moving equilibrium hypothesis sets u_* at the canopy top to be the logical variable to normalize flow statistics in z locally, which is assumed here. Variations in $\overline{w'u'}$ and σ_w in z now introduce vertical scales in ϕ_{RSL} that must be considered. The work here revealed that a ϕ_{RSL} can be derived to accommodate some of the variations in $\overline{w'u'}/u_*^2$ and σ_w/u_* as well as any imbalance between production and dissipation of turbulent kinetic energy (i.e., $P_m/\varepsilon \neq 1$) with z. The moving equilibrium hypothesis is plausible when the advection time scale $\tau_{adv} = L_x/U$ is much longer than the de-correlation or relaxation time scale of turbulence ($\tau = 2\sigma_w^2/\varepsilon$) so that turbulence equilibrates with Γ prior to being distorted by advection.[55] Here, L_x is a

characteristic length scale responsible for topographic variability and may be set to their integral scale. Thus, the moving equilibrium hypothesis requires that the integral scale of topographic variability producing $\partial\bar{P}/\partial x$ abides by

$$\frac{L_x}{L_d} \gg 2\frac{U}{u_*}\left(\frac{\sigma_w}{u_*}\right)^2. \qquad (26)$$

For the ATTO dataset analyzed here, U/u_* is of order 1–8 whereas σ_w/u_* is of order 1. Hence, the working assumption here is that $L_x/L_d \gg 1 - 20$ for $z/h \in [1, 2.2]$ (see Fig. 1). Based on digital elevation maps, $L_x = 2.5$ km around the ATTO site,[48] so the condition in Eq. (26) is reasonably satisfied for $z/h < 2.2$ when estimating $L_d \approx \kappa(z-d)$. The topographic variability at GoAmazon is not as appreciable as ATTO, and L_x/L_d is sufficiently large.

B. The length scales in the CSB model

Within the moving equilibrium hypothesis, the derivation for ϕ_{RSL} showed that the macro-scale dissipation length scale $L_d = u_*^3/\varepsilon$ emerges naturally from a co-spectral budget model. The derivation presumed that ε is the quantity that is "conserved" across the energy cascade of $E_{ww}(k)$, thereby enabling "generic" description for its shape as well as $\tau(k)$. The derivation made explicit how ϕ_{RSL} can be related to deviations in $\kappa_v(z-d)/L_d$ from unity using a co-spectral budget model. The model agrees with existing data from the ATTO, where $\overline{w'u'}$, σ_w, and P_m/ε all vary in z (Fig. 1) provided $d/h = 0.9$.[45]

Analyzing all the near-neutral stratification runs here, it was found that $L_s/h = 0.48$. Using this estimate for L_s and the complementary relation $[d + (1/2)L_s]/h = 1$[28] yields a $d/h = 0.76$. This complementary relation was derived using the drag-force centroid method for d,[25] assuming a constant leaf area density and C_d
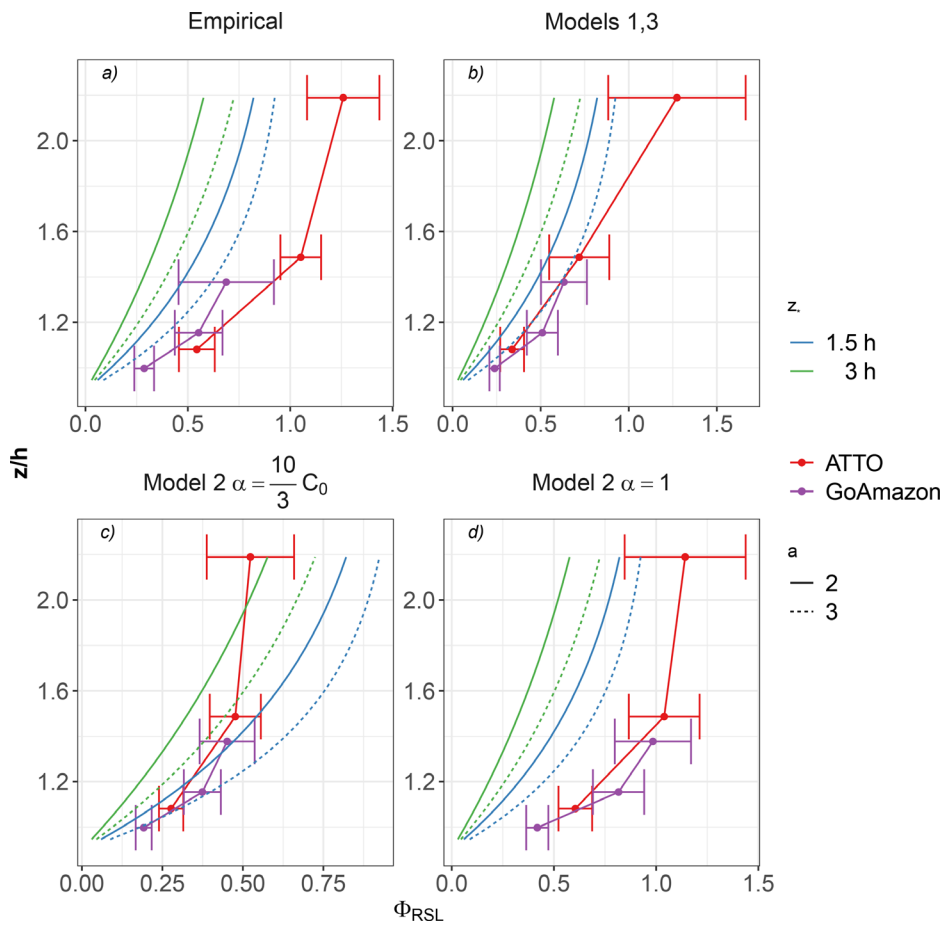
FIG. 6. The ϕ_{RSL} profiles for ATTO and GoAmazon evaluated using Eqs. (1) [panel (a)], (13) or (25) [panel (b)], and (21) for two values of α [panel (c) for $\alpha = 10C_o/3$ and panel (d) for $\alpha = 1$]. The four lines are predictions from Eq. (2) with $a = 2$ and $a = 3$ and $z_*/h = 1.5$ and $z_*/h = 3$. In the ISR, $\phi_{RSL} = 1$.

throughout, assuming the mean wind speed is monotonic and exponentially decaying within the canopy, and assuming a mixing length inside the canopy that is constant. As discussed elsewhere, those assumptions lead to an underestimate of d/h in dense urban canopies.[28] Likewise, other complementary formulations have shown that the contribution of L_s/h diminishes when the transport of K is large. In fact, in the limit when the transport of K is roughly in balance with P_m, $d/h \to 1$.[24] Thus, $d/h = 0.76$ must be viewed as a "lower-bound" on d. Setting a $d/h = 0.76$ in Eq. (1) also yields $\phi_{RSL} > 1$ at ATTO for all z/h contrary to logical expectations for the RSL.

Indirect testing of the CSB model assumptions confirmed that the peak in the pre-multiplied vertical velocity energy spectrum $kE_{ww}(k)/\sigma_w^2$ occurs around $kL_d = 0.5$ (Fig. 5). This finding also implies that this peak varies with $(\sigma_w/u_*)^3$ (Fig. 5).

VI. CONCLUSIONS

In his acceptance letter of the Rumford Medal in 1881, the physicist J. Willard Gibbs wrote that "*one of the principal objects of theoretical research is to find the point of view from which the subject appears in the greatest simplicity.*" Guided by this viewpoint, deviations from the law of the wall, a term first coined by Coles,[14] are considered for

the roughness sublayer above tall and dense forests. Near the top of vegetated canopies, modifications to the law of the wall have a long tradition of being accommodated using a dimensionless roughness sublayer correction function ϕ_{RSL} whose shape continues to draw research attention. In tall forested canopies such as the Amazon region, the experimental determination and modeling of ϕ_{RSL} may be challenging for a number of reasons. The chief one is the nonideal terrain that introduces z-dependent mean pressure gradients that then lead to variability in second-order flow velocity statistics with z at a given tower position. Using data for near-neutral atmospheric stratification collected at two sites in Amazonia, a link between the vertical velocity spectrum $E_{ww}(k)$ and ϕ_{RSL} is derived. The derivation employs a co-spectral budget (CSB) model where the friction velocity u_* is interpreted from the moving-equilibrium hypothesis to be appropriately defined at the canopy top. The CSB model reproduces the measured co-spectrum $F_{uw}(k)$ between u' and w' at all k when using the measured $E_{ww}(k)$ and when adopting a scale-dependent de-correlation time $\tau(k) = \alpha \epsilon^{-1/3} k^{-2/3}$ where $\alpha \in [1, 10C_o/3]$. Because the turbulent kinetic energy dissipation rate (ϵ) is conserved across $E_{ww}(k)$, the CSB model reveals a novel link between ϕ_{RSL} and L_{BL}/L_d, where $L_{BL} = k_v(z - d)$ is the size of attached eddies to the zero-plane displacement (d) and $L_d = u_*^3/\epsilon$ is

a dissipation length scale. The CSB model unambiguously shows that the appropriate eddy viscosity (ν_t) that applies simultaneously in the RSL and ISL is given by

$$\nu_t = \frac{1 - C_I}{C_R} \int_0^\infty \tau(k) E_{ww}(k) dk, \tag{27}$$

where C_R and C_I are constants. It will be a remiss if the analogy to the fluctuation–dissipation theorem is not pointed here. Equation (27) relates the fluctuations in velocity at all scales to a macroscopic turbulent friction or viscosity.[91] While the fluctuation–dissipation here arise from a co-spectral budget model that is in local equilibrium (stress production balances covariance destruction scale-by-scale), the $E_{ww}(k)$ contains all the complexities in turbulence associated with non-equilibrium phenomena.[92] That is, the production of $E_{ww}(k)$ occurs at scales much larger than the viscous dissipation, thereby setting an energy cascade from large to small eddies. This transfer of energy across scales is accommodated in the K41 scaling for the ISR. It is precisely the conservative (i.e., constant ε across k) nature of this cascade and the lack of equilibrium between scale-wise energy production and energy dissipation at each k that resulted in L_d being a new length scale needed to describe ν_t and thus ϕ_{RSL}. In the case where σ_w/u_* and $\overline{u'w'}/u_*^2$ are not constant in z, ϕ_{RSL} is shown to scale with $(\overline{u'w'}/u_*^2)(\sigma_w/u_*)^{-4}(L_{BL}/L_d)$. That L_d emerges as a key length scale in the RSL is independently confirmed when analyzing the eddy sizes associated with the spectral peaks in $kE_{ww}(k)$. The experiments also show that $L_d/L_s < 0.6$ for $z/h < 1.5$, $L_d/L_s = 1$ around $z/h = 1.5$, and $L_d/L_s > 1$ for $z/h > 1.5$, where L_s is the shear length scale or vorticity thickness associated with Kelvin–Helmholtz instabilities presumed to dominate coherent structures near the canopy top. It may be conjectured that when σ_w/u_*, $\overline{u'w'}/u_*^2$, and P_m/ε appreciably vary with z, L_d is an appropriate variable in the RSL and ISL when compared to L_s for modeling ϕ_{RSL} and the vertical velocity spectrum. The estimated ϕ_{RSL} derived from data near the canopy-top appear to be closer to unity when compared to those reported over agricultural crops. Future effort seeks to extend this analysis to stratified flow cases, where buoyancy production and destruction must be explicitly considered in the $E_{ww}(k)$ and $F_{uw}(k)$ budgets.

ACKNOWLEDGMENTS

AUTHOR DECLARATIONS
Conflict of Interest

The authors have no conflicts to disclose.

Author Contributions

Luca Mortarini: Data curation (lead); Formal analysis (lead); Methodology (lead); Writing – original draft (equal). **Gabriel G. Katul:** Conceptualization (lead); Formal analysis (equal); Investigation (equal); Methodology (equal); Supervision (lead); Writing – original draft (lead). **Daniela Cava:** Supervision (equal); Writing – original draft (equal). **Cleo Quaresma Dias-Junior:** Data curation (supporting); Writing – original draft (supporting). **Nelson L. Dias:** Writing – original draft (supporting). **Antonio Manzi:** Writing – original draft (supporting). **Matthias Sorgel:** Writing – original draft (supporting). **Alessandro Araujo:** Writing – original draft (supporting). **Marcelo Chamecki:** Data curation (lead); Formal analysis (lead); Writing – original draft (equal).

DATA AVAILABILITY

The data that support the findings of this study are available from the corresponding author upon reasonable request.

REFERENCES

[1]M. O. Andreae, O. C. Acevedo, A. Araùjo, P. Artaxo, C. G. G. Barbosa, H. M. J. Barbosa, J. Brito, S. Carbone, X. Chi, B. B. L. Cintra, N. F. da Silva, N. L. Dias, C. Q. Dias-Júnior, F. Ditas, R. Ditz, A. F. L. Godoi, R. H. M. Godoi, M. Heimann, T. Hoffmann, J. Kesselmeier, T. Könemann, M. L. Krüger, J. V. Lavric, A. O. Manzi, A. P. Lopes, D. L. Martins, E. F. Mikhailov, D. Moran-Zuloaga, B. W. Nelson, A. C. Nölscher, D. Santos Nogueira, M. T. F. Piedade, C. Pöhlker, U. Pöschl, C. A. Quesada, L. V. Rizzo, C.-U. Ro, N. Ruckteschler, L. D. A. S. M. de Oliveira Sá, C. B. Sales, R. M. N. dos Santos, J. Saturno, J. Schöngart, M. Sörgel, C. M. d Souza, R. A. F. de Souza, H. Su, N. Targhetta, J. Tóta, I. Trebs, S. Trumbore, A. van Eijck, D. Walter, Z. Wang, B. Weber, J. Williams, J. Winderlich, F. Wittmann, S. Wolff, and A. M. Y. Serrano, "The amazon tall tower observatory (atto): Overview of pilot measurements on ecosystem ecology, meteorology, trace gases, and aerosols," Atmos. Chem. Phys. **15**, 10723–10776 (2015).

[2]M. Raupach, "Conditional statistics of Reynolds stress in rough-wall and smooth-wall turbulent boundary layers," J. Fluid Mech. **108**, 363–382 (1981).

[3]J. Finnigan, "Turbulence in plant canopies," Annu. Rev. Fluid Mech. **32**, 519–571 (2000).

[4]Y. Brunet, "Turbulent flow in plant canopies: Historical perspective and overview," Boundary Layer Meteorol. **177**, 315–364 (2020).

[5]G. B. Bonan, E. G. Patton, IN. Harman, K. W. Oleson, J. J. Finnigan, Y. Lu, and E. A. Burakowski, "Modeling canopy-induced turbulence in the Earth system: A unified parameterization of turbulent exchange within plant canopies and the roughness sublayer (CLM-ml v0)," Geosci. Model Dev. **11**, 1467–1496 (2018).

[6]J. Lee, J. Hong, Y. Noh, and P. A. Jiménez, "Implementation of a roughness sublayer parameterization in the weather research and forecasting model (WRF version 3.7.1) and its evaluation for regional climate simulations," Geosci. Model Dev. **13**, 521–536 (2020).

[7]M. Raupach and A. Thom, "Turbulence in and above plant canopies," Annu. Rev. Fluid Mech. **13**, 97–129 (1981).

[8]W. Brutsaert, *Hydrology: An Introduction* (Cambridge University Press, Cambridge, 2005), p. 605.

[9]M. Kadivar, D. Tormey, and G. McGranaghan, "A review on turbulent flow over rough surfaces: Fundamentals and theories," Int. J. Thermofluids **10**, 100077 (2021).

[10]P. Cellier and Y. Brunet, "Flux-gradient relationships above tall plant canopies," Agric. For. Meteorol. **58**, 93–117 (1992).

[11]W. Physick and J. Garratt, "Incorporation of a high-roughness lower boundary into a mesoscale model for studies of dry deposition over complex terrain," Boundary Layer Meteorol. **74**, 55–71 (1995).

[12]F. C. Bosveld, "Derivation of fluxes from profiles over a moderately homogeneous forest," Boundary Layer Meteorol. **84**, 289–327 (1997).

[13]L. Prandtl, *Essentials of Fluid Dynamics: With Applications to Hydraulics Aeronautics, Meteorology, and Other Subjects* (Hafner Publishing Company, 1952).

[14]D. E. Coles, "The law of the wake in the turbulent boundary layer," J. Fluid Mech. **1**, 191–226 (1956).

[15]J. Garratt, "Flux profile relations above tall vegetation," Q. J. R. Meteorol. Soc. **104**, 199–211 (1978).

[16]M. Raupach, "Anomalies in flux-gradient relationships over forest," Boundary Layer Meteorol. **16**, 467–486 (1979).

[17]J. Garratt, "Surface influence upon vertical profiles in the atmospheric near-surface layer," Q. J. R. Meteorol. Soc. **106**, 803–819 (1980).

[18]K. De Ridder, "Bulk transfer relations for the roughness sublayer," Boundary Layer Meteorol. **134**, 257–267 (2010).

[19]J. Graefe, "Roughness layer corrections with emphasis on SVAT model applications," Agric. For. Meteorol. **124**, 237–251 (2004).

[20]K. Weligepolage, A. Gieske, C. van der Tol, J. Timmermans, and Z. Su, "Effect of sub-layer corrections on the roughness parameterization of a Douglas fir forest," Agric. For. Meteorol. **162**, 115–126 (2012).

[21]A. Wenzel, N. Kalthoff, and V. Horlacher, "On the profiles of wind velocity in the roughness sublayer above a coniferous forest," Boundary Layer Meteorol. **84**, 219–230 (1997).

[22]J. Arnqvist and H. Bergström, "Flux-profile relation with roughness sublayer correction," Q. J. R. Meteorol. Soc. **141**, 1191–1197 (2015).

[23]S. Bailey, M. Vallikivi, M. Hultmark, and A. Smits, "Estimating the value of von Kármán constant in turbulent pipe flow," J. Fluid Mech. **749**, 79–98 (2014).

[24]A. Sogachev and M. Kelly, "On displacement height, from classical to practical formulation: Stress, turbulent transport and vorticity considerations," Boundary Layer Meteorol. **158**, 361–381 (2016).

[25]P. Jackson, "On the displacement height in the logarithmic velocity profile," J. Fluid Mech. **111**, 15–25 (1981).

[26]D. Poggi, A. Porporato, L. Ridolfi, J. Albertson, and G. Katul, "The effect of vegetation density on canopy sub-layer turbulence," Boundary Layer Meteorol. **111**, 565–587 (2004).

[27]W. Brutsaert, *Evaporation into the Atmosphere: Theory, History and Applications* (Springer Science and Business Media, 1982), Vol. 1.

[28]Q. Li and G. Katul, "Bridging the urban canopy sublayer to aerodynamic parameters of the atmospheric surface layer," Boundary Layer Meteorol. **185**, 35–61 (2022).

[29]G. Gioia and P. Chakraborty, "Spectral derivation of the classic laws of wall-bounded turbulent flows," Proc. R. Soc. A: Math. Phys. Eng. Sci. **473**, 20170354 (2017).

[30]A. S. Monin and A. M. Obukhov, "Basic laws of turbulent mixing in the surface layer of the atmosphere," Contrib. Geophys. Inst. Acad. Sci. USSR **151**, e187 (1954).

[31]O. Coceal and S. Belcher, "A canopy model of mean winds through urban areas," Q. J. R. Meteorol. Soc. **130**, 1349–1372 (2004).

[32]C. Manes, D. Poggi, and L. Ridolfi, "Turbulent boundary layers over permeable walls: Scaling and near-wall structure," J. Fluid Mech. **687**, 141–170 (2011).

[33]I. N. Harman and J. J. Finnigan, "A simple unified theory for flow in the canopy and roughness sublayer," Boundary Layer Meteorol. **123**, 339–363 (2007).

[34]Z. Mo, C.-H. Liu, H.-L. Chow, M.-K. Lam, Y.-H. Lok, S.-W. Ma, F.-L. Wong, and P.-Y. Yip, "Roughness sublayer over vegetation canopy: A wind tunnel study," Agric. For. Meteorol. **316**, 108880 (2022).

[35]M. R. Raupach, J. J. Finnigan, and Y. Brunet, "Coherent eddies and turbulence in vegetation canopies: The mixing-layer analogy," Boundary Layer Meteorol. **78**, 351–382 (1996).

[36]M. Mölder, A. Grelle, A. Lindroth, and S. Halldin, "Flux-profile relationships over a boreal forest—Roughness sublayer corrections," Agric. For. Meteorol. **98**, 645–658 (1999).

[37]J. Kaimal and J. J. Finnigan, *Atmospheric Boundary Layer Flows: Their Structure and Measurement* (Oxford University Press, 1994).

[38]I. N. Harman, "The role of roughness sublayer dynamics within surface exchange schemes," Boundary Layer Meteorol. **142**, 1–20 (2012).

[39]W. Sadeh, J. Cermak, and T. Kawatani, "Flow over high roughness elements," Boundary Layer Meteorol. **1**, 321–344 (1971).

[40]S. Pope, *Turbulent Flows* (Cambridge University Press, Cambridge, UK, 2000), p. 771.

[41]J. J. Finnigan, R. H. Shaw, and E. G. Patton, "Turbulence structure above a vegetation canopy," J. Fluid Mech. **637**, 387–424 (2009).

[42]S. Dupont and E. G. Patton, "On the influence of large-scale atmospheric motions on near-surface turbulence: Comparison between flows over low-roughness and tall vegetation canopies," Boundary Layer Meteorol. **184**, 195–230 (2022).

[43]A. Thom, J. Stewart, H. Oliver, and J. Gash, "Comparison of aerodynamic and energy budget estimates of fluxes over a pine forest," Q. J. R. Meteorol. Soc. **101**, 93–105 (1975).

[44]W. C. Allee, "Measurement of environmental factors in the tropical rain-forest of panama," Ecology **7**, 273–302 (1926).

[45]C. Q. Dias-Júnior, N. L. Dias, R. M. N. dos Santos, M. Sörgel, A. Araújo, A. Tsokankunku, F. Ditas, R. A. de Santana, C. von Randow, M. Sá *et al.*, "Is there a classical inertial sublayer over the amazon forest?," Geophys. Res. Lett. **46**, 5614–5622, https://doi.org/10.1029/2019GL083237 (2019).

[46]T. L. Chor, N. L. Dias, A. Araújo, S. Wolff, E. Zahn, A. Manzi, I. Trebs, M. O. Sá, P. R. Teixeira, and M. Sörgel, "Flux-variance and flux-gradient relationships in the roughness sublayer over the amazon forest," Agric. For. Meteorol. **239**, 213–222 (2017).

[47]E. Zahn, N. L. Dias, A. Araújo, L. D. Sá, M. Sörgel, I. Trebs, S. Wolff, and A. Manzi, "Scalar turbulent behavior in the roughness sublayer of an amazonian forest," Atmos. Chem. Phys. **16**, 11349–11366 (2016).

[48]M. Chamecki, L. S. Freire, N. L. Dias, B. Chen, C. Q. Dias-Junior, L. A. Toledo Machado, M. Sörgel, A. Tsokankunku, and A. C. de Araújo, "Effects of vegetation and topography on the boundary layer structure above the amazon forest," J. Atmos. Sci. **77**, 2941–2957 (2020).

[49]P. Davidson and P.-Å. Krogstad, "A universal scaling for low-order structure functions in the log-law region of smooth-and rough-wall boundary layers," J. Fluid Mech. **752**, 140–156 (2014).

[50]M. Chamecki, N. L. Dias, S. T. Salesky, and Y. Pan, "Scaling laws for the longitudinal structure function in the atmospheric surface layer," J. Atmos. Sci. **74**, 1127–1147 (2017).

[51]Y. Pan and M. Chamecki, "A scaling law for the shear-production range of second-order structure functions," J. Fluid Mech. **801**, 459–474 (2016).

[52]K. Ghannam, G. G. Katul, E. Bou-Zeid, T. Gerken, and M. Chamecki, "Scaling and similarity of the anisotropic coherent eddies in near-surface atmospheric turbulence," J. Atmos. Sci. **75**, 943–964 (2018).

[53]G. G. Katul, A. Porporato, C. Manes, and C. Meneveau, "Co-spectrum and mean velocity in turbulent boundary layers," Phys. Fluids **25**, 091702 (2013).

[54]D. Cava and G. Katul, "On the scaling laws of the velocity-scalar cospectra in the canopy sublayer above tall forests," Boundary Layer Meteorol. **145**, 351–367 (2012).

[55]S. Belcher, N. Jerram, and J. Hunt, "Adjustment of a turbulent boundary layer to a canopy of roughness elements," J. Fluid Mech. **488**, 369–398 (2003).

[56]D. Poggi, C. Krug, and G. G. Katul, "Hydraulic resistance of submerged rigid vegetation derived from first-order closure models," Water Resour. Res. **45**, W10442, https://doi.org/10.1029/2008WR007373 (2009).

[57]H. Tennekes and J. Lumley, *A First Course in Turbulence* (MIT Press, Cambridge, MA, 1972), p. 300.

[58]A. Yaglom, "Similarity laws for constant-pressure and pressure-gradient turbulent wall flows," Annu. Rev. Fluid Mech. **11**, 505–540 (1979).

[59]B. A. Kader and A. M. Yaglom, "Similarity treatment of moving-equilibrium turbulent boundary layers in adverse pressure gradients," J. Fluid Mech. **89**, 305–342 (1978).

[60]G. Katul, C.-I. Hsieh, D. Bowling, K. Clark, N. Shurpali, A. Turnipseed, J. Albertson, K. Tu, D. Hollinger, B. Evans *et al.*, "Spatial variability of turbulent

fluxes in the roughness sublayer of an even-aged pine forest," Boundary Layer Meteorol. **93**, 1–28 (1999).

[61]B. Chen, M. Chamecki, and G. G. Katul, "Effects of topography on in-canopy transport of gases emitted within dense forests," Q. J. R. Meteorol. Soc. **145**, 2101–2114 (2019).

[62]K.-S. Choi and J. L. Lumley, "The return to isotropy of homogeneous turbulence," J. Fluid Mech. **436**, 59–84 (2001).

[63]P. Durbin, "A Reynolds stress model for near-wall turbulence," J. Fluid Mech. **249**, 465–498 (1993).

[64]B. Launder, G. Reece, and W. Rodi, "Progress in the development of a Reynolds-stress turbulence closure," J. Fluid Mech. **68**, 537–566 (1975).

[65]K. Hanjalić and B. Launder, "Reassessment of modeling turbulence via Reynolds averaging: A review of second-moment transport strategy," Phys. Fluids **33**, 091302 (2021).

[66]W. Bos, H. Touil, L. Shao, and J. Bertogli, "On the behavior of the velocity-scalar cross correlation spectrum in the inertial range," Phys. Fluids **16**, 3818–3823 (2004).

[67]G. Katul, D. Li, M. Chamecki, and E. Bou-Zeid, "Mean scalar concentration profile in a sheared and thermally stratified atmospheric surface layer," Phys. Rev. E **87**, 023004 (2013).

[68]D. Besnard, F. Harlow, R. Rauenzahn, and C. Zemach, "Spectral transport model for turbulence," Theor. Comput. Fluid Dyn. **8**, 1–35 (1996).

[69]A. Ayet, G. Katul, A. Bragg, and J.-L. Redelsperger, "Scalewise return to isotropy in stratified boundary layer flows," J. Geophys. Res.: Atmos. **125**, e2020JD032732, http://dx.doi.org/10.1029/2020JD032732 (2020).

[70]D. Li and G. G. Katul, "On the linkage between the $k^{-5/3}$ spectral and $k^{-7/3}$ cospectral scaling in high-Reynolds number turbulent boundary layers," Phys. Fluids **29**, 065108 (2017).

[71]J. Lumley, "Similarity and the turbulent energy spectrum," Phys. Fluids **10**, 855–858 (1967).

[72]S. Saddoughi and S. Veeravalli, "Local isotropy in turbulent boundary layers at high Reynolds number flow," J. Fluid Mech. **268**, 333–372 (1994).

[73]G. Katul, C. Geron, C. Hsieh, B. Vidakovic, and A. Guenther, "Active turbulence and scalar transport near the land-atmosphere interface," J. Appl. Meteorol. **37**, 1533–1546 (1998).

[74]U. Högström, J. Hunt, and A.-S. Smedman, "Theory and measurements for turbulence spectra and variances in the atmospheric neutral surface layer," Boundary Layer Meteorol. **103**, 101–124 (2002).

[75]P. Drobinski, P. Carlotti, R. K. Newsom, R. M. Banta, R. C. Foster, and J.-L. Redelsperger, "The structure of the near-neutral atmospheric surface layer," J. Atmos. Sci. **61**, 699–714 (2004).

[76]M. B. Siqueira and G. G. Katul, "An analytical model for the distribution of co_2 sources and sinks, fluxes, and mean concentration within the roughness sublayer," Boundary Layer Meteorol. **135**, 31–50 (2010).

[77]J. D. Fuentes, M. Chamecki, R. M. N. Dos Santos, C. Von Randow, P. C. Stoy, G. Katul, D. Fitzjarrald, A. Manzi, T. Gerken, A. Trowbridge *et al.*, "Linking meteorology, turbulence, and air chemistry in the amazon rain forest," Bull. Am. Meteorol. Soc. **97**, 2329–2342 (2016).

[78]L. Freire, T. Gerken, J. Ruiz-Plancarte, D. Wei, J. Fuentes, G. Katul, N. Dias, O. Acevedo, and M. Chamecki, "Turbulent mixing and removal of ozone within an amazon rainforest canopy," J. Geophys. Res.: Atmos. **122**, 2791–2811, https://doi.org/10.1002/2016JD026009 (2017).

[79]S. Dupont and E. G. Patton, "Influence of stability and seasonal canopy changes on micrometeorology within and above an orchard canopy: The chats experiment," Agric. For. Meteorol. **157**, 11–29 (2012).

[80]K. Everard, G. Katul, G. Lawrence, A. Christen, and M. Parlange, "Sweeping effects modify Taylor's frozen turbulence hypothesis for scalars in the roughness sublayer," Geophys. Res. Lett. **48**, e2021GL093746, http://dx.doi.org/10.1029/2021GL093746 (2021).

[81]D. Charuchittipan and J. Wilson, "Turbulent kinetic energy dissipation in the surface layer," Boundary Layer Meteorol. **132**, 193–204 (2009).

[82]D. Poggi, G. Katul, and J. Albertson, "Momentum transfer and turbulent kinetic energy budgets within a dense model canopy," Boundary Layer Meteorol. **111**, 589–614 (2004).

[83]S. T. Salesky, G. G. Katul, and M. Chamecki, "Buoyancy effects on the integral length scales and mean velocity profile in atmospheric surface layer flows," Phys. Fluids **25**, 105101 (2013).

[84]R. Van Hout, W. Zhu, L. Luznik, J. Katz, J. Kleissl, and M. Parlange, "PIV measurements in the atmospheric boundary layer within and above a mature corn canopy. I. Statistics and energy flux," J. Atmos. Sci. **64**, 2805–2824 (2007).

[85]B. Chen and M. Chamecki, "Turbulent kinetic energy budgets over gentle topography covered by forests," J. Atmos. Sci. **80**, 91–109 (2023).

[86]A. Townsend, *The structure of Turbulent Shear Flow* (Cambridge University Press, 1976).

[87]A. Perry and C. Abell, "Asymptotic similarity of turbulence structures in smooth- and rough-walled pipes," J. Fluid Mech. **79**, 785–799 (1977).

[88]G. Katul and C.-R. Chu, "A theoretical and experimental investigation of energy-containing scales in the dynamic sublayer of boundary-layer flows," Boundary Layer Meteorol. **86**, 279–312 (1998).

[89]B. Kader and A. Yaglom, "Spectra and correlation functions of surface layer atmospheric turbulence in unstable thermal stratification," in *Turbulence and Coherent Structures* (Springer, 1991), pp. 387–412.

[90]V. Nikora, "Origin of the '−1' spectral law in wall-bounded turbulence," Phys. Rev. Lett. **83**, 734 (1999).

[91]N. Goldenfeld and H.-Y. Shih, "Turbulence as a problem in non-equilibrium statistical mechanics," J. Stat. Phys. **167**, 575–594 (2017).

[92]K. Sreenivasan, "Fluid turbulence," Rev. Mod. Phys. **71**, S383–S395 (1999).